CHAPTER IV
RESULTS AND DISCUSSION

4.1 Catalyst Preparation

This part reports the washcoating results of ceramic monolith used as a catalytic support and also some information of all library members.

4.1.1 Monolith Washcoating

The original and bit monoliths were investigated for their surface morphologies using SEM, as shown in Figure 4.1. Some surface roughness has been observed after the acid biting expected to enhance the attachment between monolithic wall and alumina slurry. After bit monoliths were dipped into γ-Al_2O_3 slurry and calcined at 500°C, their alumina coated thicknesses were also estimated by SEM. Figure 4.2 illustrates the results at the different magnifications of the washcoated monolith. It was indicated that γ-Al_2O_3 was coated as a layer on the monolithic walls with the thickness of around 30-35 μm. The SEM result of bare monolith, as shown in Figure 4.3, also confirms the existing of additional γ-Al_2O_3 layers onto monolithic walls.
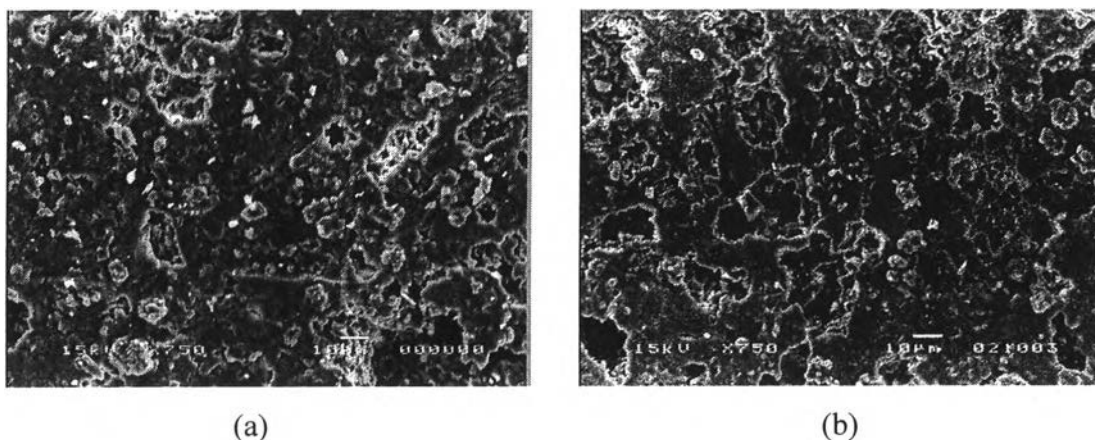

(a)   (b)

Figure 4.1 SEM images of (a) original ceramic monolith, and (b) bit monolith (dipped with 2.5%wt acetic acid solution for around 2 min).

(a)

(b)

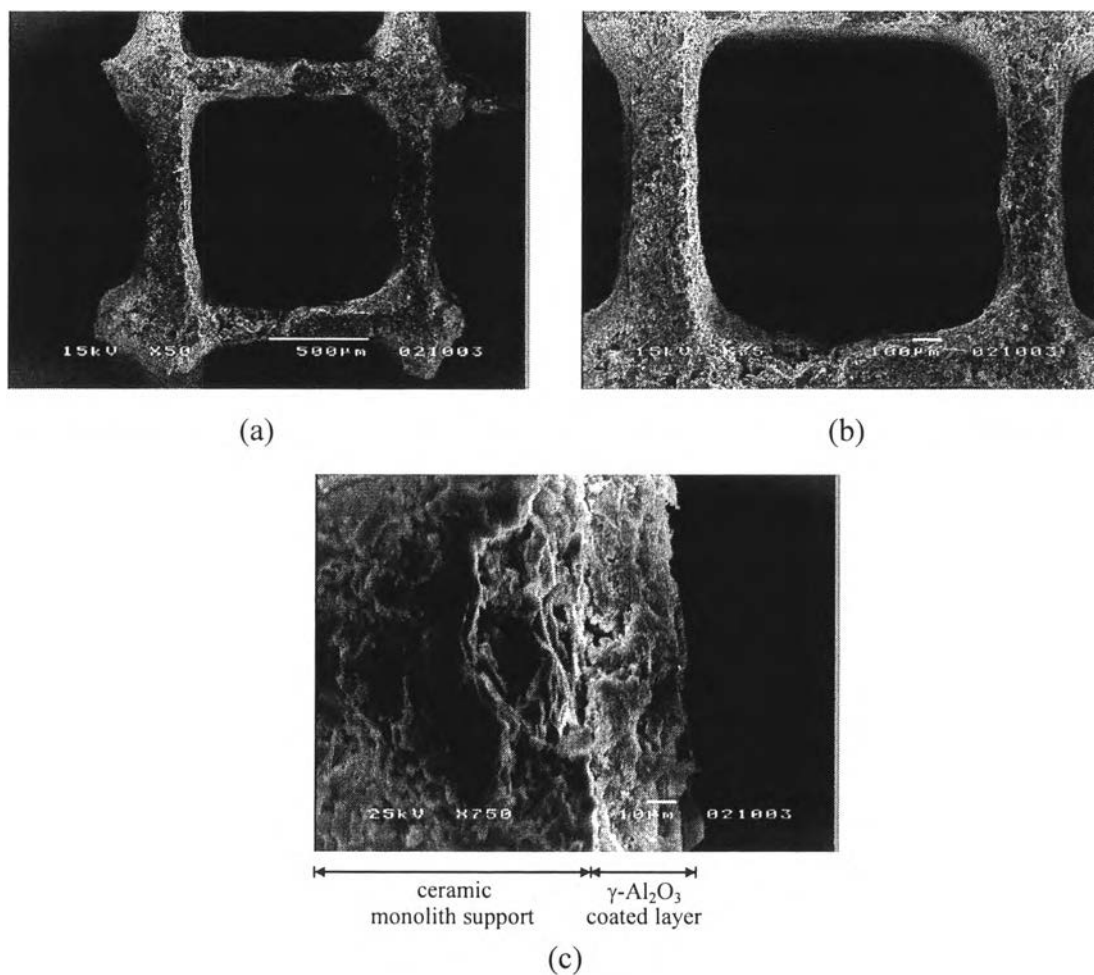ceramic
monolith support

γ-Al₂O₃
coated layer

(c)

Figure 4.2 SEM images of γ-Al$_2$O$_3$ washcoated monolith with the magnifications of (a) 50, (b) 75, and (c) 750 times.
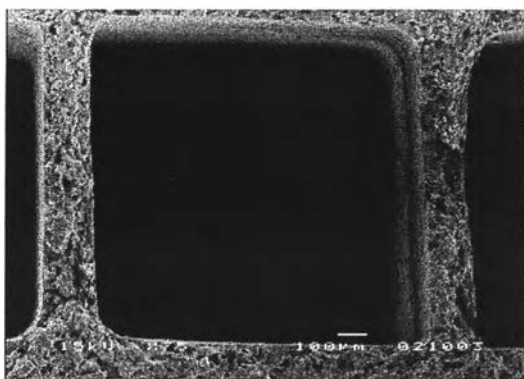

Figure 4.3 SEM image of bare ceramic monolith.

4.1.2 Library I: Catalysts for Studying the Effect of Calcination Step

Eight monolithic catalysts were selected to observe the effect of calcination related to alumina phase. There are three main categories: i) unloaded catalysts, ii) palladium-based catalysts (both bi- and tri- elements), and iii) platinum-based catalysts. All of them are identified and also listed in Table 4.1.

Table 4.1 Catalyst formulations prepared by incipient wetness method to achieve 5% total loading for studying the effect of catalyst preparation

No.	Catalyst	Relative ratio of elemental loading (%)			Remark
		Pd	Pt	La	
1	CM	-	-	-	Bare Monolith
2	C22	-	-	-	Washcoated Monolith
3	C19A	80	20	-	Method A (Pd-based)
4	C19B	80	20	-	Method B (Pd-based)
5	C17A	60	20	20	Method A (Pd-based)
6	C17B	60	20	20	Method B (Pd-based)
7	C02A	-	80	20	Method A (Pt-based)
8	C02B	-	80	20	Method B (Pt-based)

Note: Method A: washcoated monolith was calcined at 500°C and re-calcined at 900°C for 3 hrs after metal loading.

Method B: washcoated monolith was calcined at 900°C and re-calcined at 900°C for 3 hrs after metal loading.

The XRD patterns in Figure 4.4 indicate that Method A generates γ-alumina phase while mixed γ- and δ-alumina phases are achieved from Method B (both patterns were matched with the XRD references: PDF No. 29-63, and 46-1131, respectively).
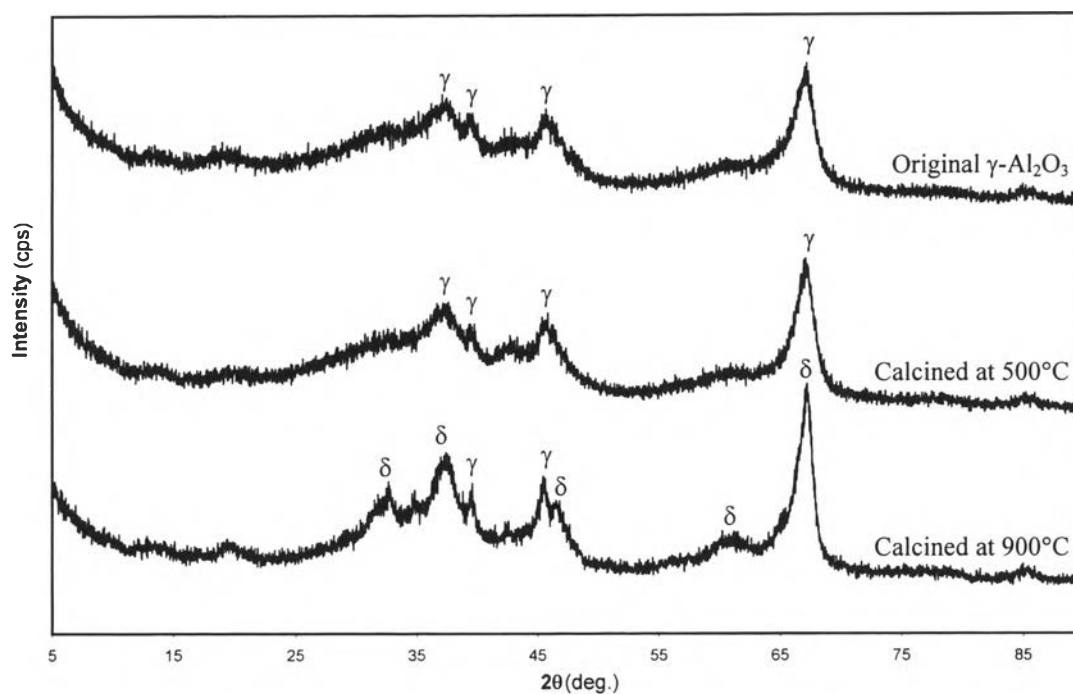
Figure 4.4 XRD patterns of original γ-Al_2O_3, calcined γ-Al_2O_3 at 500 and 900°C for 3 hrs.

4.1.3 Library II: Catalysts for Studying the Effect of Loading Amount

Eight palladium supported γ-Al_2O_3 washcoated ceramic monoliths were prepared with different total loading amounts with an appropriate calcination step from the previous experiment. All of them are identified and also listed in Table 4.2.

Table 4.2 Catalyst formulations prepared by incipient wetness method for studying the effect of loading amount

No.	Catalyst	Pd loading (%wt)	No.	Catalyst	Pd loading (%wt)
1	ML1	1%	5	ML5	7%
2	ML2	2%	6	ML6	8%
3	ML3	4%	7	ML7	10%
4	ML4	5%	8	ML8	12%

4.1.4 Library III: Catalysts for Studying the Effect of Using Pd, Pt, and La in mono-, bi-, and tri-elements System

Twenty-one catalysts loaded with Pd, Pt, and La simultaneously by a 20% interval, in mono-, bi-, and tri-elements system were prepared according to tertiary diagram. The calcination step and total loading were used as the appropriate conditions received from the previous study. All of them are identified and also listed in Table 4.3, and Figure 4.5.

Table 4.3 Catalyst formulations for studying the feasibility of using Pd, Pt, and La in mono-, bi-, and tri-elements system

No	Catalyst	Relative ratio of elemental loading[†] (%)			No	Catalyst	Relative ratio of elemental loading[†] (%)		
		Pd	Pt	La			Pd	Pt	La
1	C01[a]	-	100	-	13	C13[c]	40	40	20
2	C02[b]	-	80	20	14	C14[c]	40	20	40
3	C03[b]	-	60	40	15	C15[b]	40	-	60
4	C04[b]	-	40	60	16	C16[b]	60	40	-
5	C05[b]	-	20	80	17	C17[c]	60	20	20
6	C06[a]	-	-	100	18	C18[b]	60	-	40
7	C07[b]	20	80	-	19	C19[b]	80	20	-
8	C08[c]	20	60	20	20	C20[b]	80	-	20
9	C09[c]	20	40	40	21	C21[a]	100	-	-
10	C10[c]	20	20	60	22	C22[*]	-	-	-
11	C11[b]	20	-	80	23	C23[‡]	-	-	-
12	C12[b]	40	60	-					

Note: [†] with 5% total elemental loading
[a] single-element catalysts
[b] catalysts in the bi-element system: Pt/La, Pa/La, or Pd/Pt
[c] catalysts in the tri-element system of Pd, Pt and La
[*] unloaded catalyst (γ-Al_2O_3 washcoated ceramic monolith)
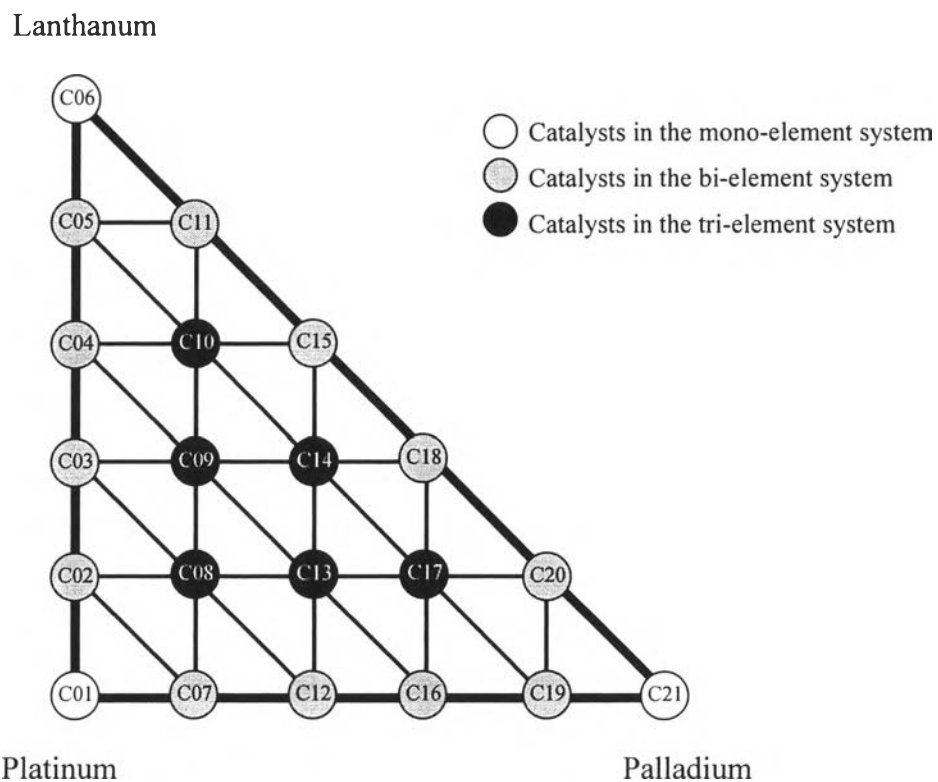[‡] quartz wool to represent the non-catalytic case

Lanthanum

Figure 4.5 A rightangled triangle tertiary diagram representing a systematic arrangement of catalysts in Library III.
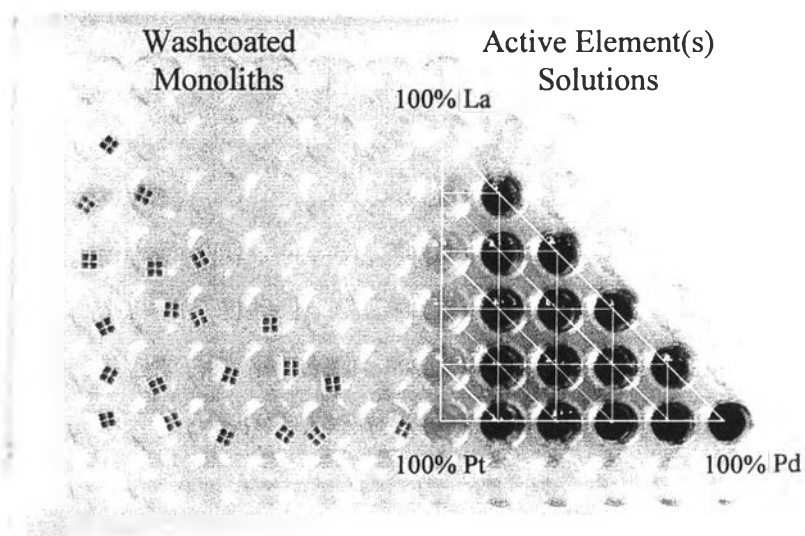

Figure 4.6 A picture of washcoated monoliths (in the left-hand-side) to be impregnated with active element(s) solutions (in the right-hand-side).

4.2 Catalytic Activity Screening

This section shows the activity of all catalysts in the libraries. The activity testing was investigated under the simulated operating conditions of a small turbine unit at 1 atm. The conditions were 2% methane in air with 1 m/s linear velocity at fixed different given temperatures in each experiment.

4.2.1 Activity Screening of Library I: Study of the Effect of Calcination Step

The experiments were performed at 650°C to observe some differences between two preparation methods related to alumina phase. The compositions of all catalyst formulations used in this study are displayed in Table 4.1. From GC data, 100% selectivity was achieved with conversion as illustrated in Figure 4.7.
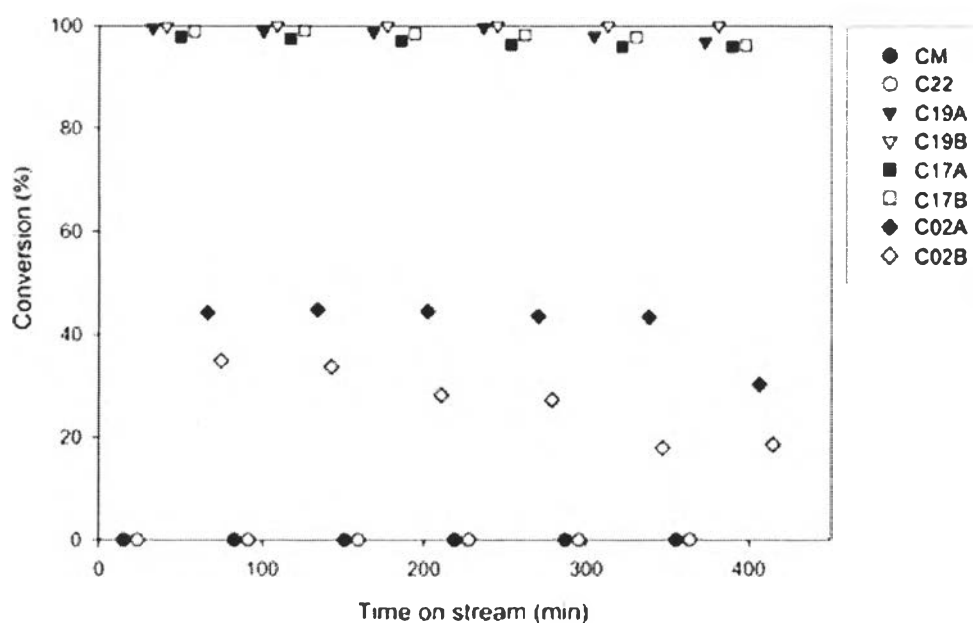
Figure 4.7 Methane conversion of catalysts in Library I from the activity screening using eight tubular flow reactors (filled symbols indicate the catalysts prepared from Method A while the opened symbols indicate the catalysts prepared from Method B).

The results indicate that Pd-based catalysts has a high potential to combust a lean mixture of methane since some of them have almost 100% conversion and 100% selectivity. Moreover, no significant difference was observed in a long period when the different calcination steps were applied to prepare Pd-based catalysts. On the other hand, loading Pt-based elements on γ-phase alumina, using Method A, gave a higher activity when compared to the other one from Method B. Therefore, Method A, which washcoated monoliths were calcined at 500°C before re-calcination at 900°C after metal loading, is suggested to be the appropriate condition for preparing the methane combustion catalysts.

4.2.1 Activity Screening of Library II: Study of the Effect of Loading Amount

The appropriate preparation condition suggested from the previous test was used to produce a catalyst library for studying the effect of loading amount. Eight different loaded catalysts were investigated for their combustion activity under three different temperatures: 350, 400, and 450°C, as shown in Figures 4.8 to 4.10.

Figure 4.8 represents the methane conversion at 350°C. The screening results showed the needs of palladium to be loaded in higher amounts at this temperature since the activity of all catalysts was still low, around 10-15% conversion. However, the results at 450°C, as illustrated in Figure 4.10, evidenced that it was not necessary to load metals in very high amounts because most of catalysts with about 4% loading can give almost complete combustion of methane.

In Figure 4.9, the methane conversion at 400°C is exhibited, and also confirmed the conclusion that it was not necessary to load metals in very high amounts since almost the same activity, around 25-35% conversion, were observed for all catalysts containing about 4% loading or higher in a long period of time. Therefore, 5% is suggested to be an optimum loading on the accounts of high activity assured and metals cost benefited.
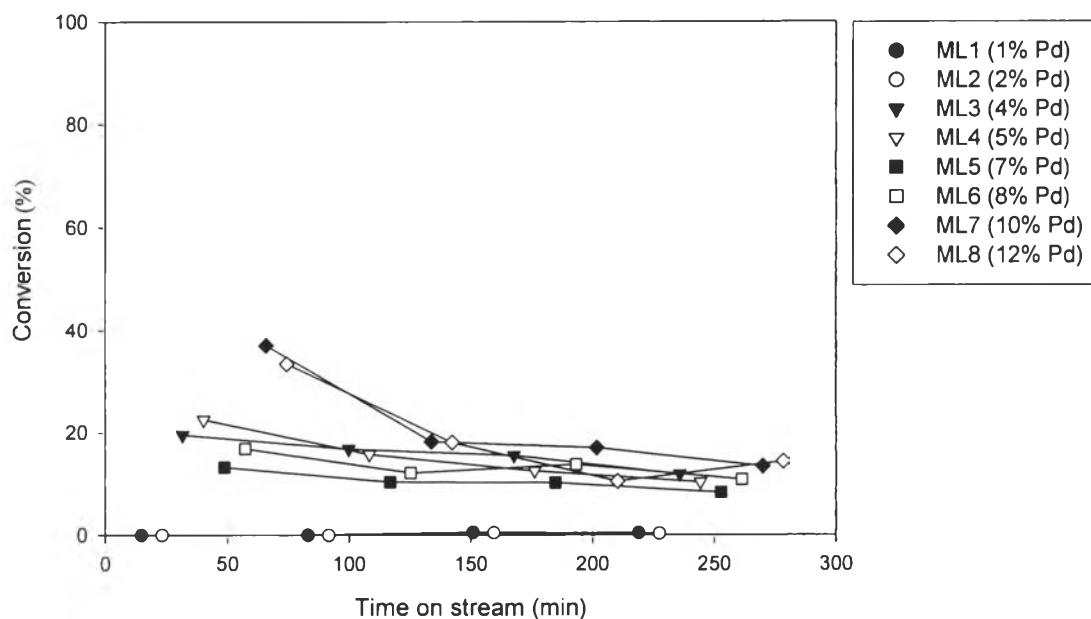
Figure 4.8 Methane conversion of catalysts in Library II from the activity screening at 350°C with eight tubular flow reactors.
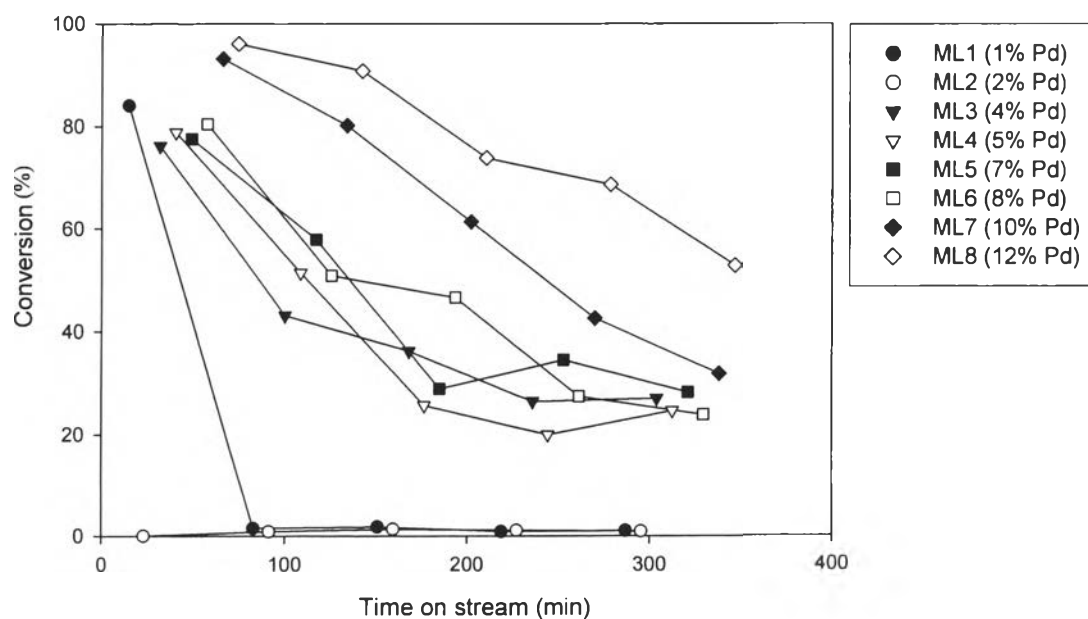

Figure 4.9 Methane conversion of catalysts in Library II from the activity screening at 400°C with eight tubular flow reactors.
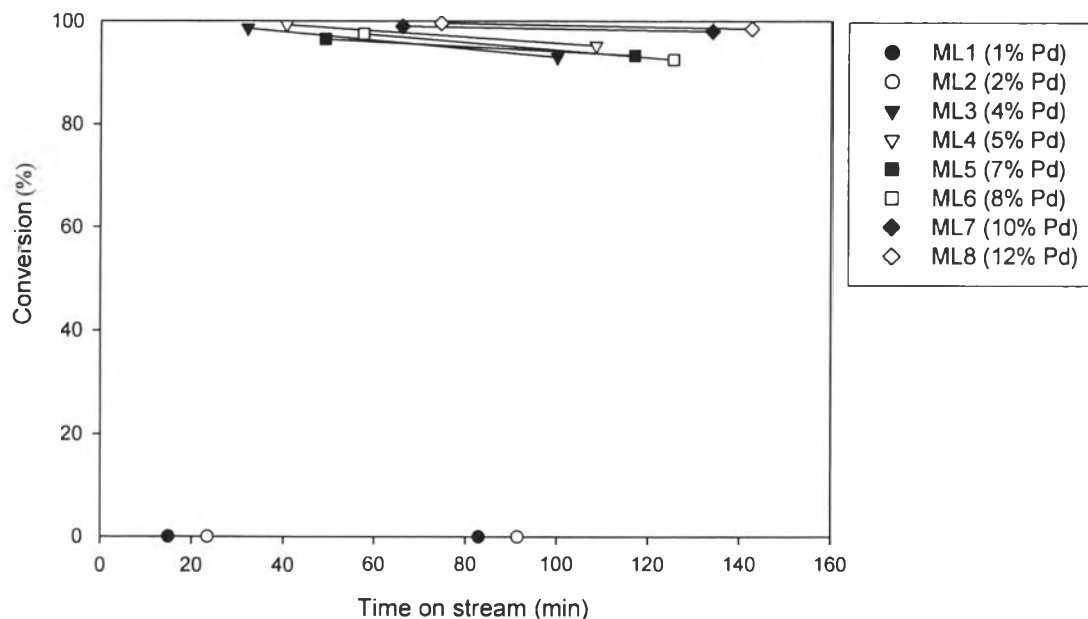
Figure 4.10 Methane conversion of catalysts in Library II from the activity screening at 450°C with eight tubular flow reactors.

4.2.1 Activity Screening of Library III: Study of the Effect of Using Pd, Pt, and La in mono-, bi-, and tri-elements System

Twenty-one catalysts were prepared in mono-, bi-, and tri-elements system according to the appropriate preparation condition and the optimum loading from the previous two experiments. Their compositions are shown in Table 4.3 and Figure 4.5. For studying the feasibility of multi-element system, the experiments were designed to perform within the range 400-600°C with a 50°C increment, which is the applicable range of low-temperature catalyst in a catalytic combustor. Another experiment at 800°C was also investigated to study the feasibility of using the catalysts in severe conditions, e.g. the overheating condition.

Conversions along time-on-stream at different temperatures of all catalyst members are illustrated in Figures 4.11 to 4.33 by the identified order, respectively.
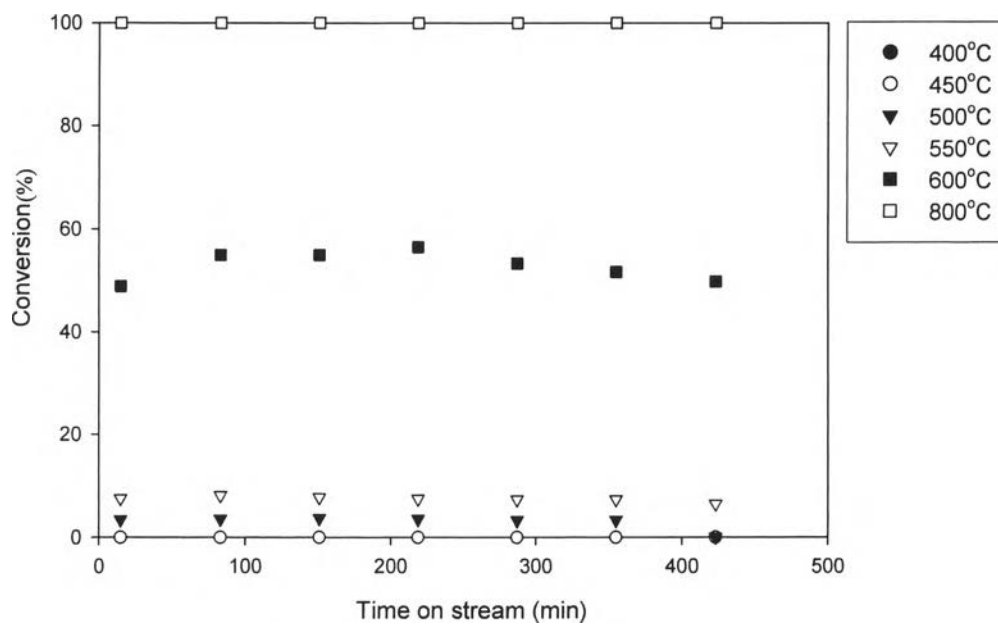
Figure 4.11 Conversion at different temperatures of 5% pure Pt loaded monolithic catalyst (C01).
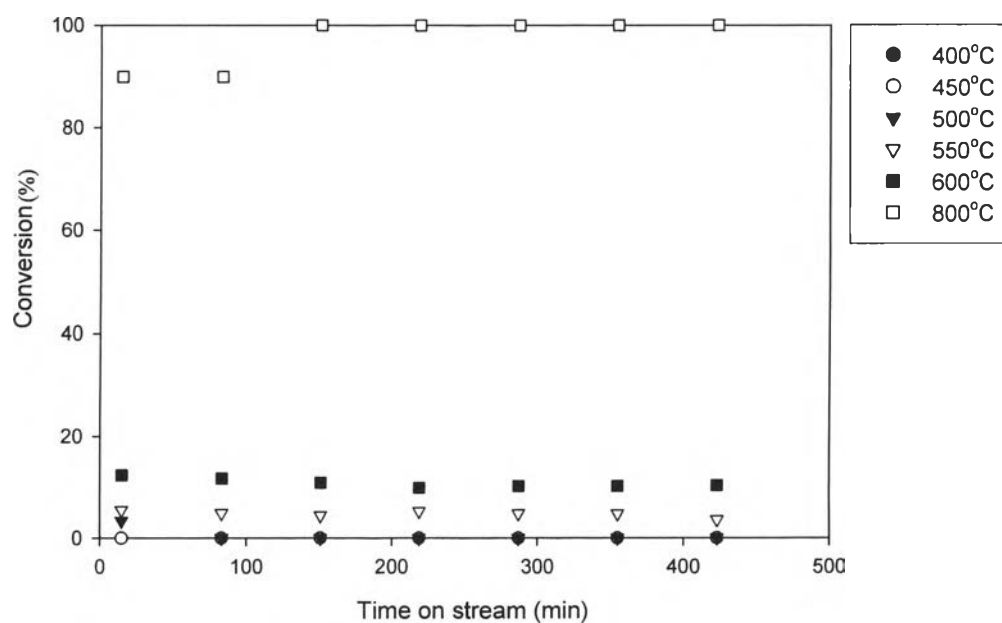

Figure 4.12 Conversion at different temperatures of 5% loaded monolithic catalyst whose loading was relatively composed of 80% Pt and 20% La (C02).
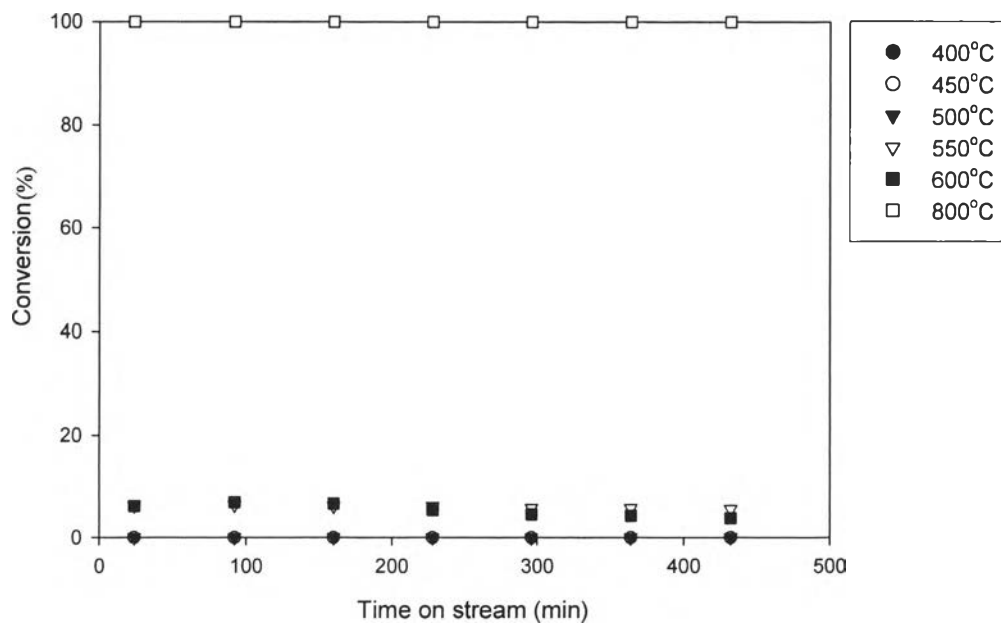
Figure 4.13 Conversion at different temperatures of 5% loaded monolithic catalyst whose loading was relatively composed of 60% Pt and 40% La (C03).
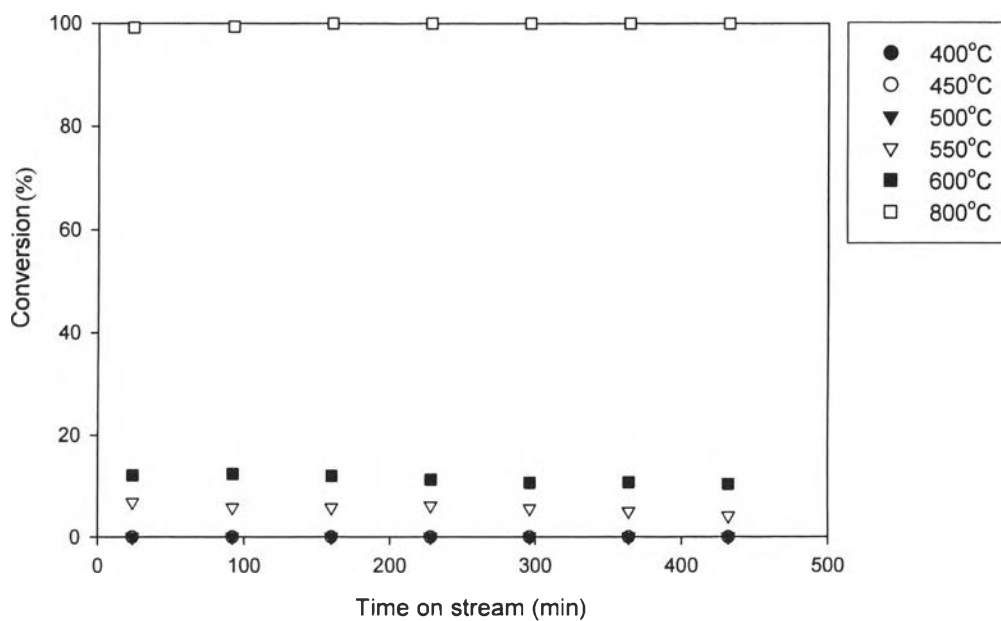

Figure 4.14 Conversion at different temperatures of 5% loaded monolithic catalyst whose loading was relatively composed of 40% Pt and 60% La (C04).
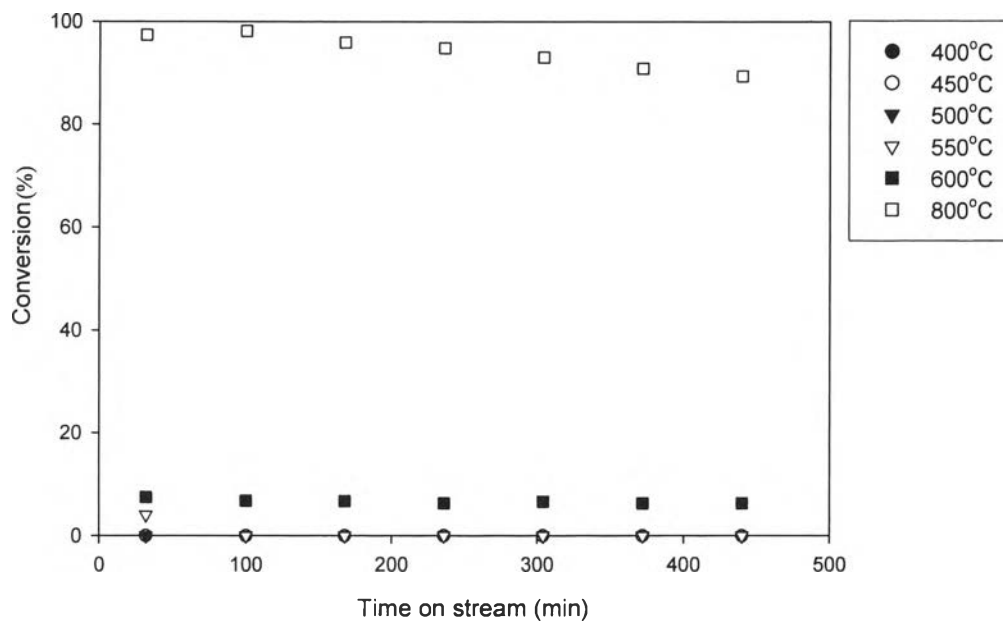
Figure 4.15 Conversion different temperatures of 5% loaded monolithic catalyst whose loading was relatively composed of 20% Pt and 80% La (C05).
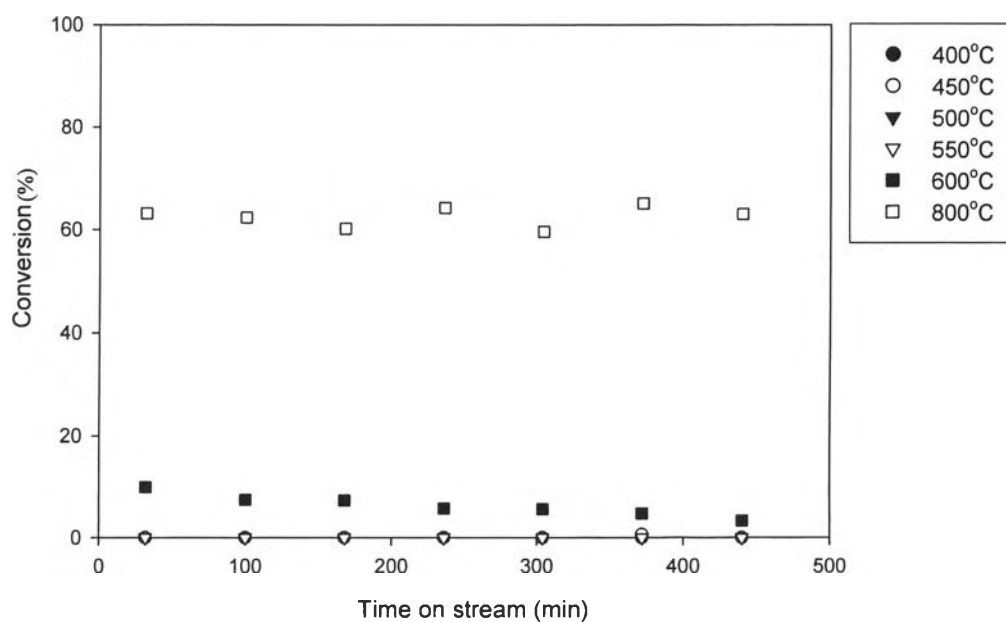

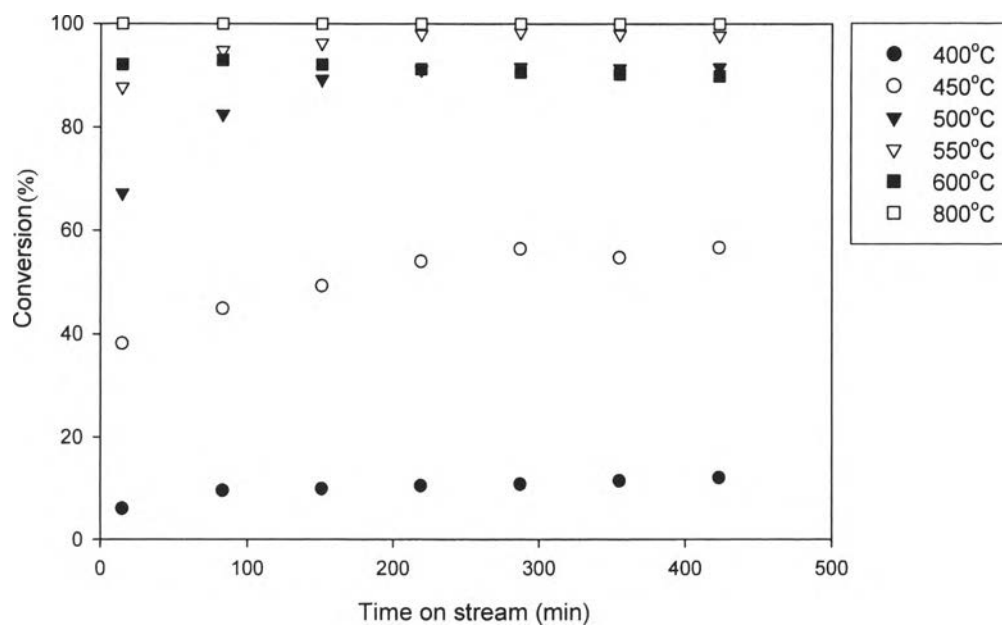**Figure 4.16** Conversion at different temperatures of 5% pure La loaded monolithic catalyst (C06).

Figure 4.17 Conversion at different temperatures of 5% loaded monolithic catalyst whose loading was relatively composed of 20% Pd and 80% Pt (C07).
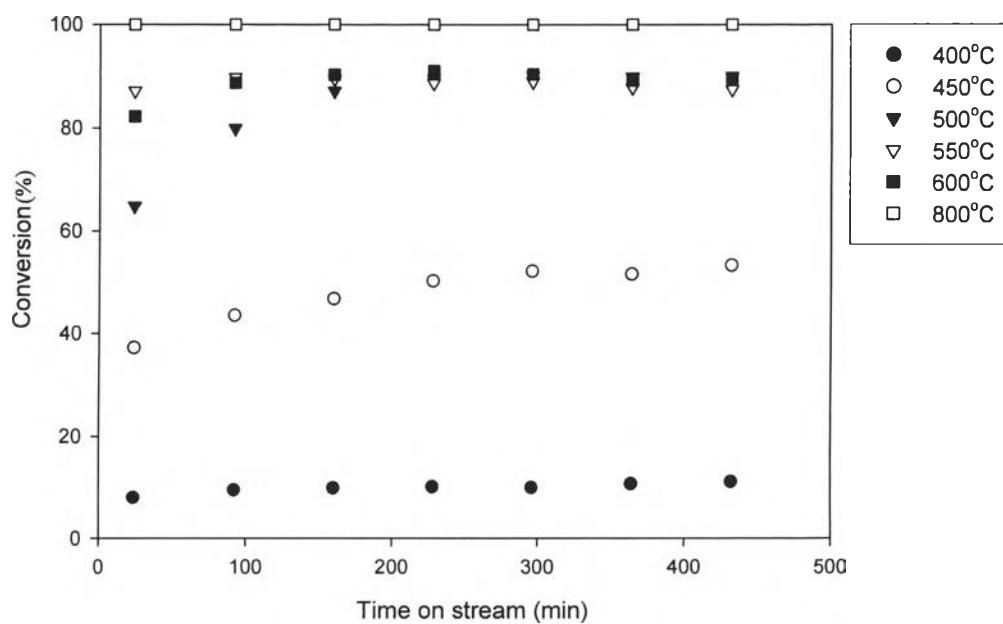

Figure 4.18 Conversion at different temperatures of 5% loaded monolithic catalyst whose loading was relatively composed of 20% Pd, 60% Pt, and 20% La (C08).
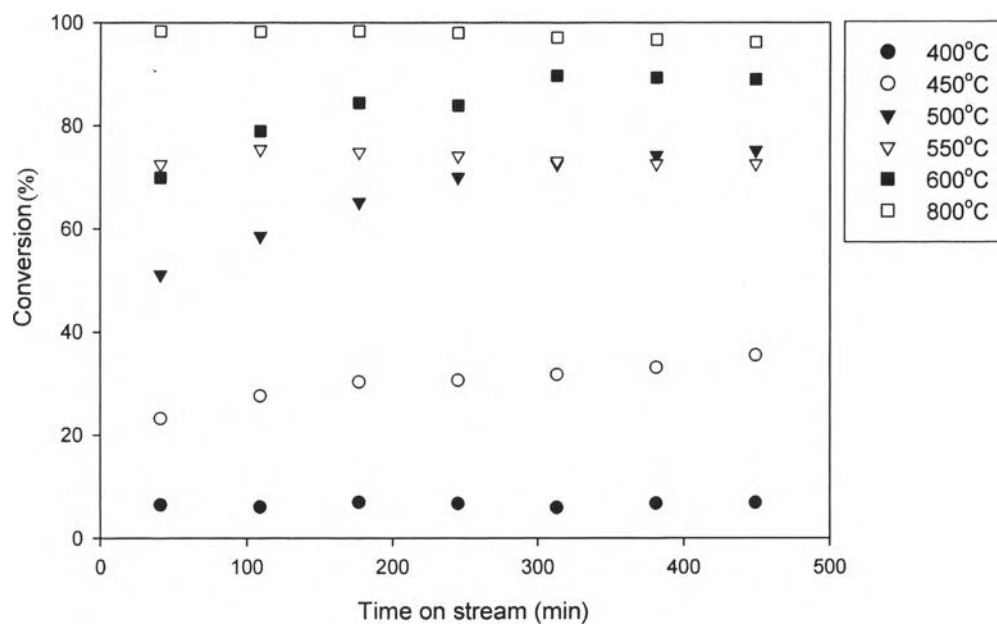
Figure 4.19 Conversion at different temperatures of 5% loaded monolithic catalyst whose loading was relatively composed of 20% Pd, 40% Pt, and 40% La (C09).
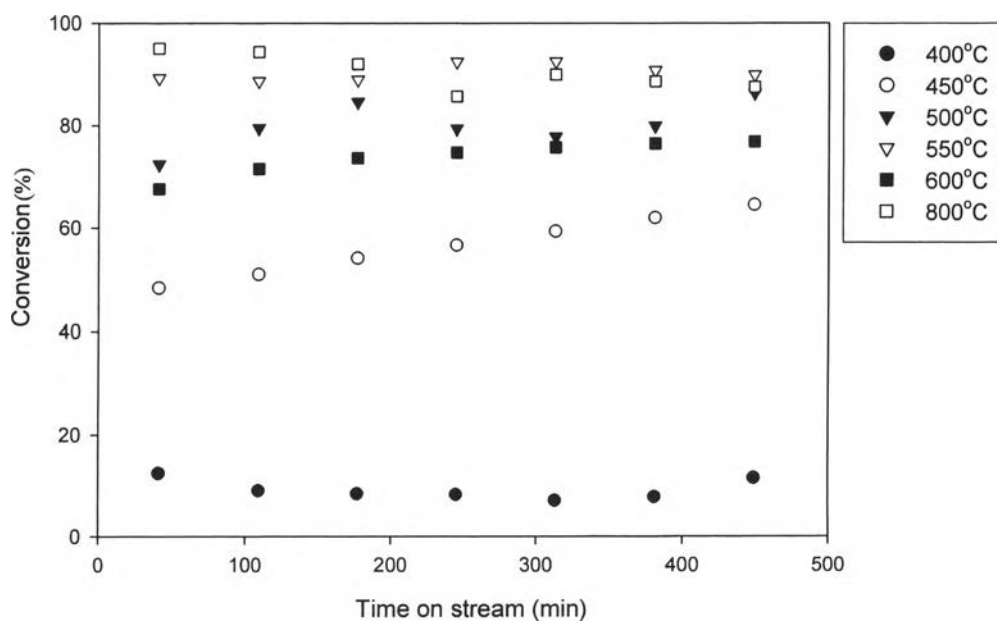

Figure 4.20 Conversion at different temperatures of 5% loaded monolithic catalyst whose loading was relatively composed of 20% Pd, 20% Pt, and 60% La (C10).
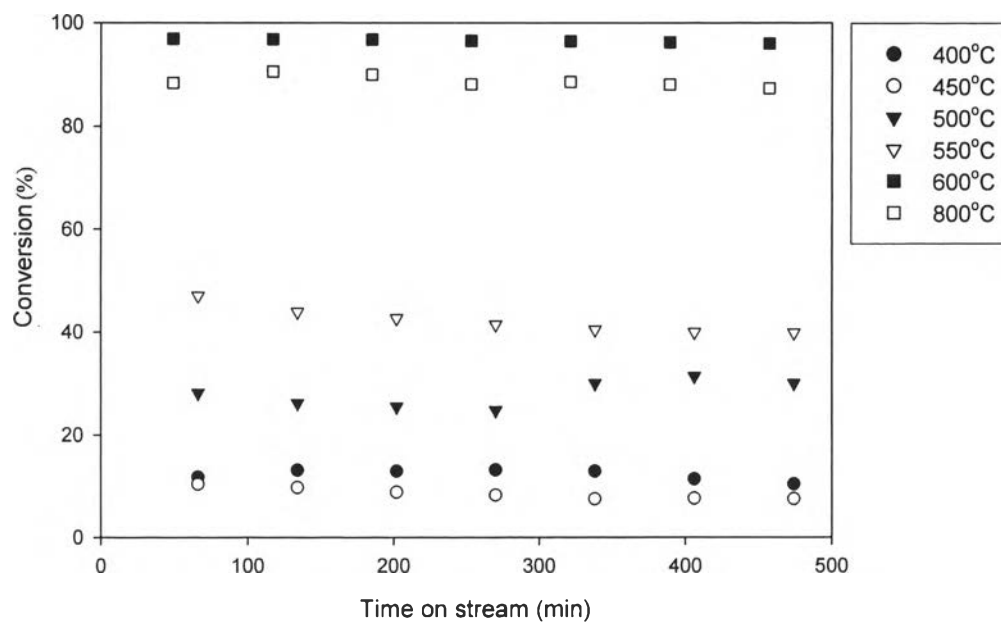
Figure 4.21 Conversion at different temperatures of 5% loaded monolithic catalyst whose loading was relatively composed of 20% Pd and 80% La (C11).

Figure 4.22 Conversion at different temperatures of 5% loaded monolithic catalyst whose loading was relatively composed of 40% Pd and 60% Pt (C12).

Figure 4.23 Conversion at different temperatures of 5% loaded monolithic catalyst whose loading was relatively composed of 40% Pd, 40% Pt, and 20% La (C13).

Figure 4.24 Conversion at different temperatures of 5% loaded monolithic catalyst whose loading was relatively composed of 40% Pd, 20% Pt, and 40% La (C14).
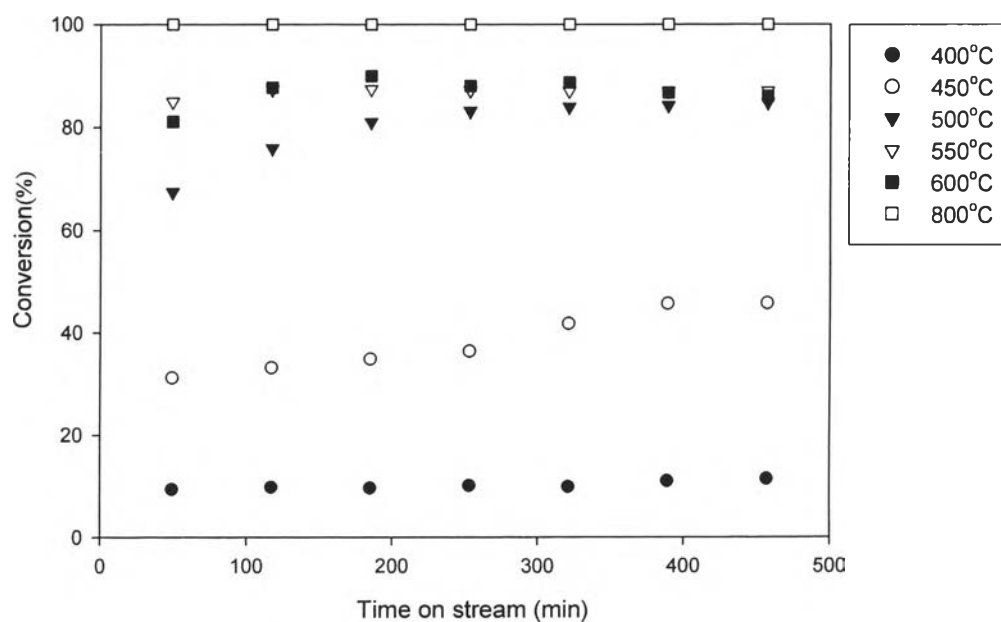
Figure 4.25 Conversion at different temperatures of 5% loaded monolithic catalyst whose loading was relatively composed of 40% Pd and 60% La (C15).

Figure 4.26 Conversion at different temperatures of 5% loaded monolithic catalyst whose loading was relatively composed of 60% Pd and 40% Pt (C16).
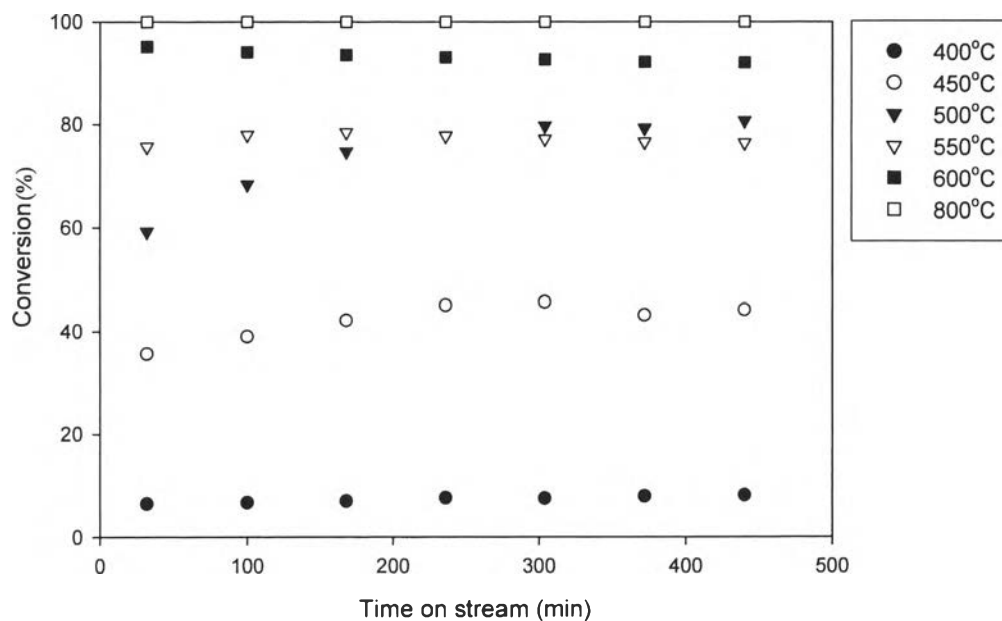
Figure 4.27 Conversion at different temperatures of 5% loaded monolithic catalyst whose loading was relatively composed of 60% Pd, 20% Pt, and 20% La (C17).
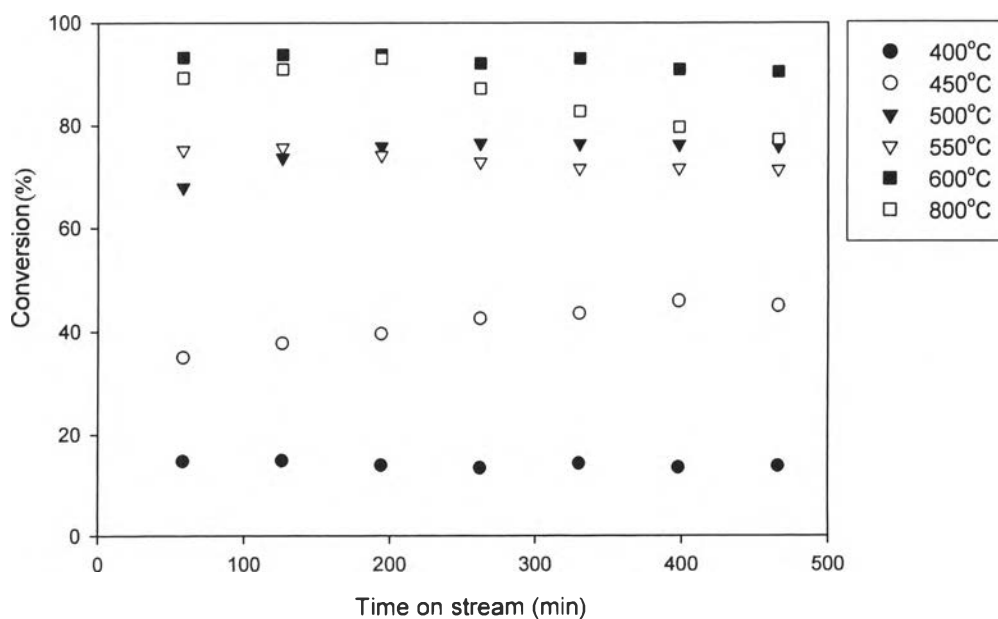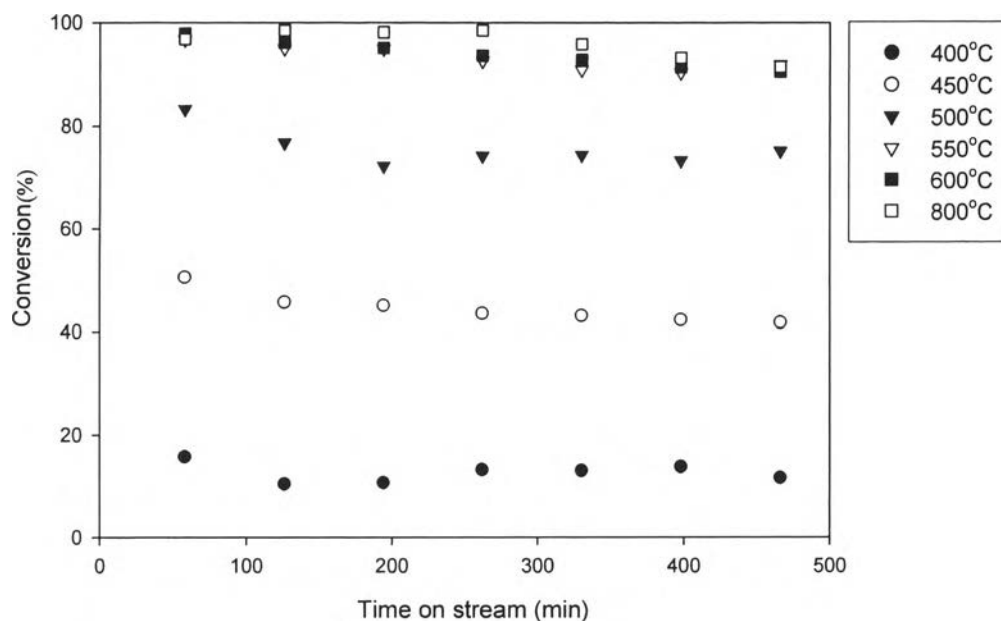

Figure 4.28 Conversion at different temperatures of 5% loaded monolithic catalyst whose loading was relatively composed of 60% Pd and 40% La (C18).
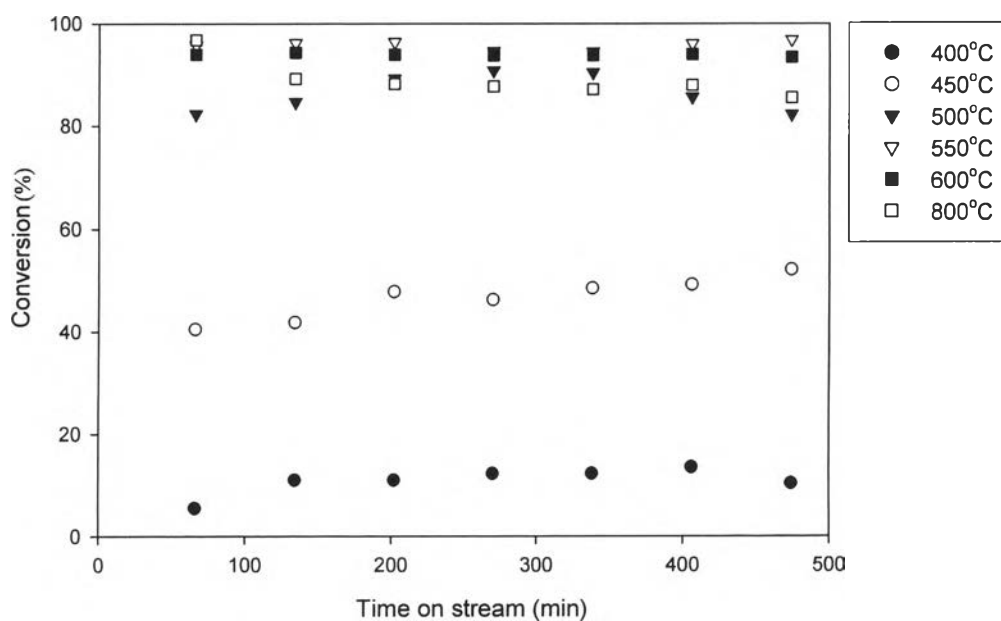
Figure 4.29 Conversion at different temperatures of 5% loaded monolithic catalyst whose loading was relatively composed of 80% Pd and 20% Pt (C19).

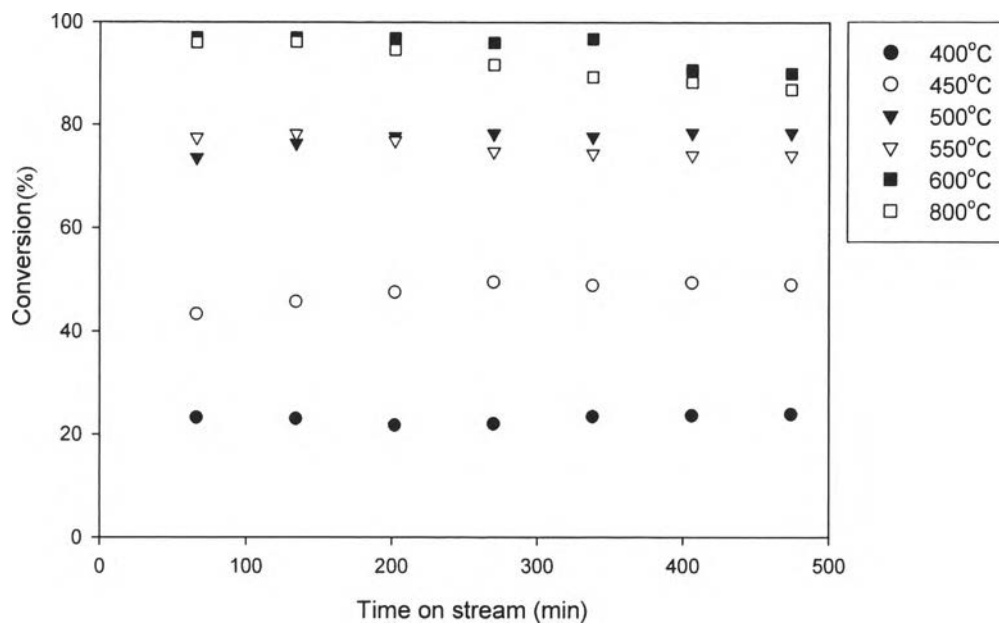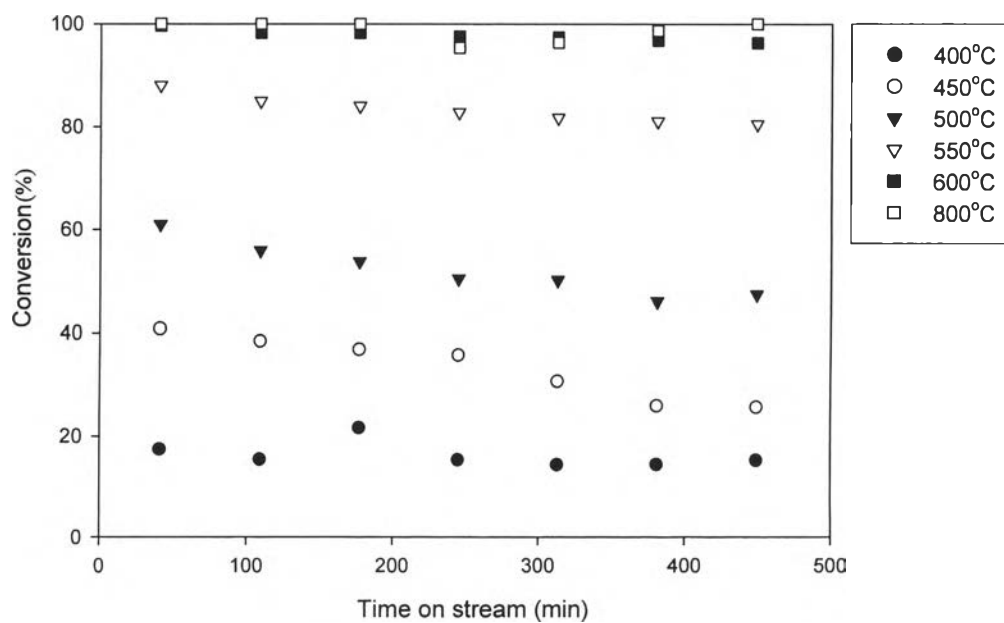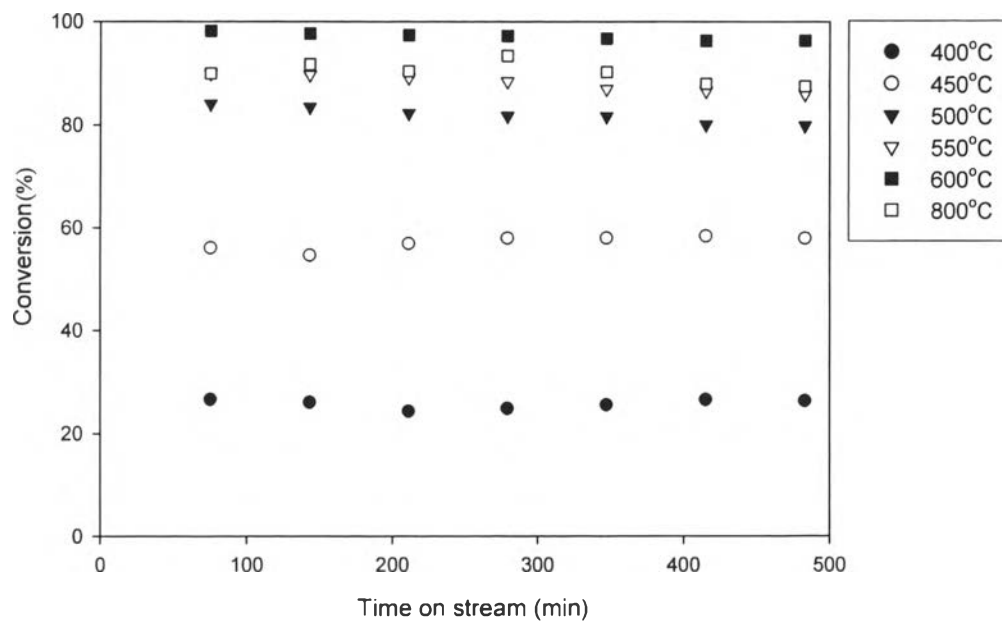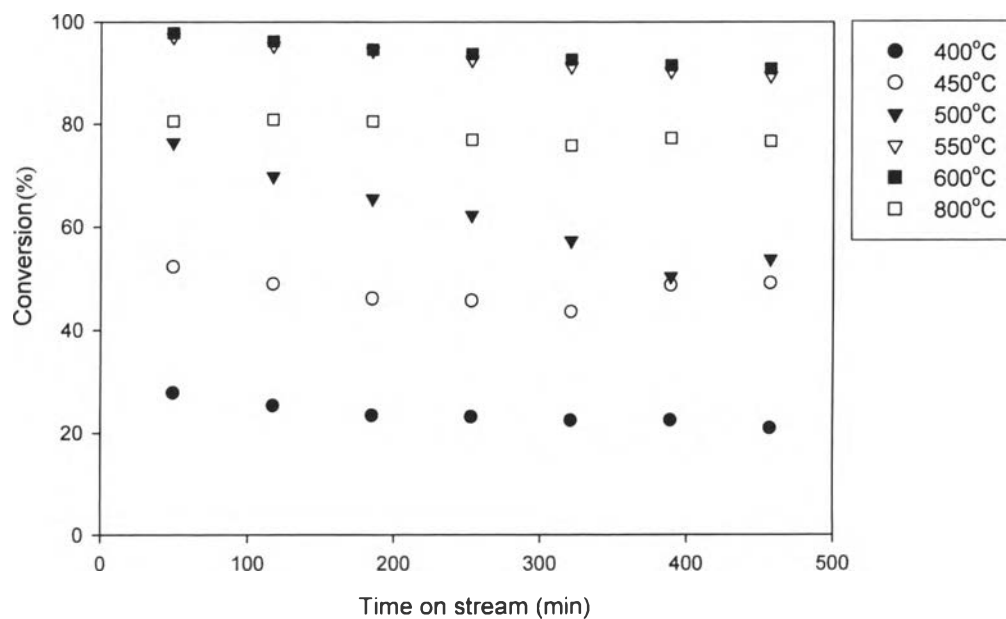**Figure 4.30** Conversion at different temperatures of 5% loaded monolithic catalyst whose loading was relatively composed of 80% Pd and 20% La (C20).
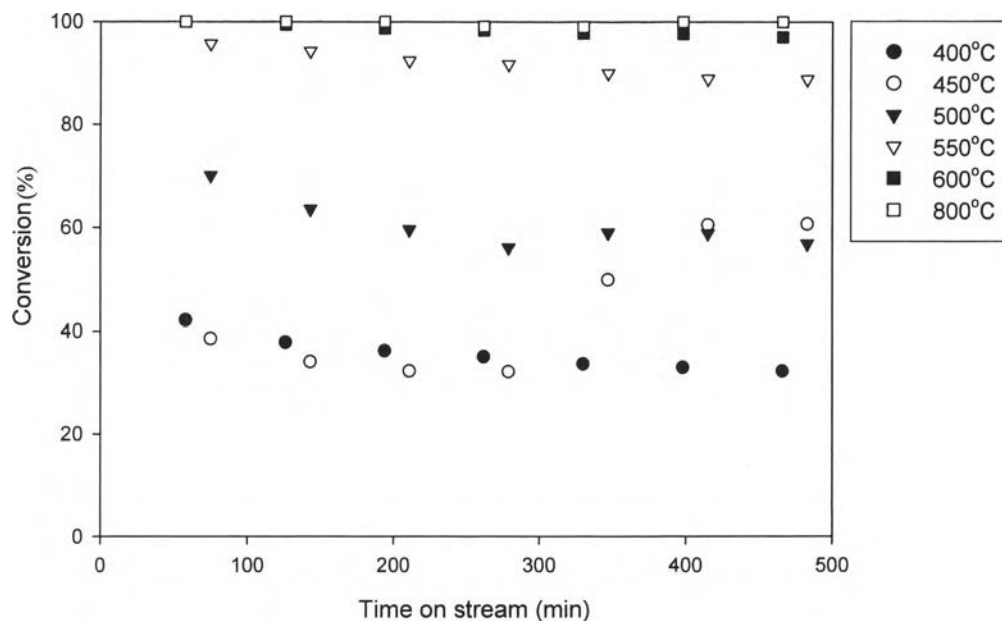
Figure 4.31 Conversion at different temperatures of 5% pure Pd loaded monolithic catalyst (C21).
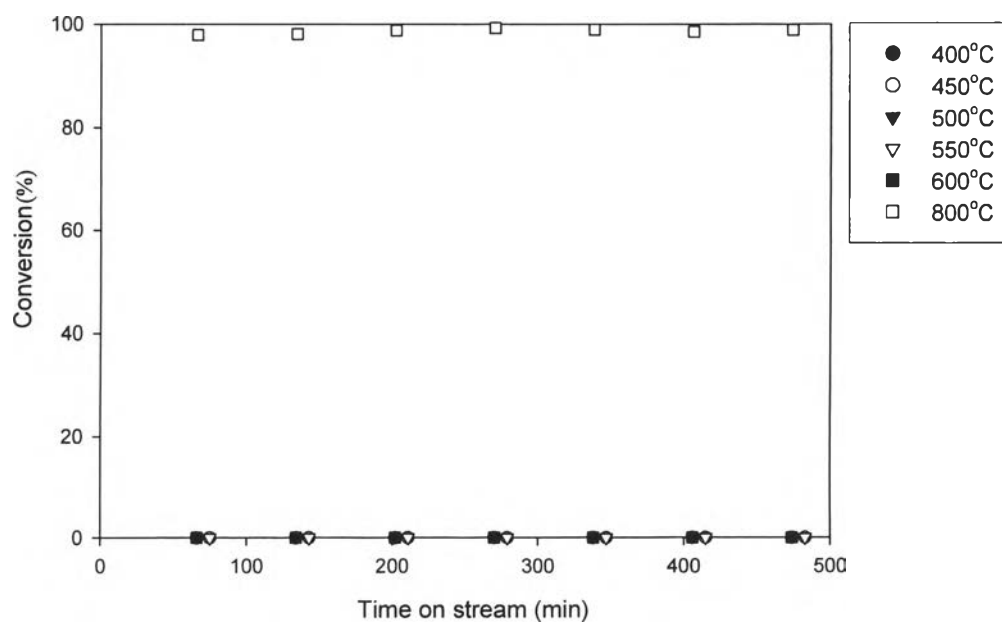
Figure 4.32 Conversion of washcoated monolithic catalyst (without loaded element).
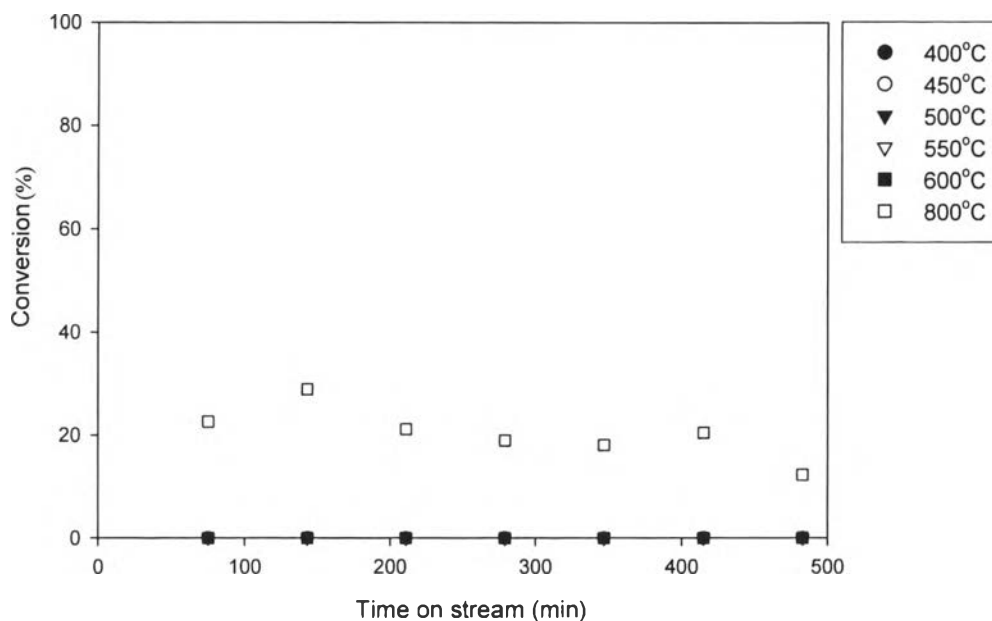
Figure 4.33 Conversion of methane without catalyst (homogeneous combustion).

From the results, all catalytic activities between 400-600°C were observed to increase with the reaction temperatures, which indicated the surface kinetic control mechanism. At the higher temperature of about 800°C, some homogeneous combustion are expected to occur since at least 12% conversion of methane has been observed from the reaction without catalyst. This phenomenon also resulted in almost 100% conversion of all loaded catalysts at this high temperature.

For the carbon dioxide selectivity, it was observed that all methane combusted on catalytic surface was completely converted to only carbon dioxide. That means only total combustion of methane has been occurred, which resulted in 100% selectivity.

The contour plots in rightangled tertiary diagram of all catalysts, according to Figure 4.5, at the different temperatures were constructed with the steady state conversion. The colors in this diagram indicate the different conversion and active zone for each selected temperature and also indicate the lead formulations. The plots are shown in Figures 4.34 and 4.35.

Figure 4.34 Contour plots of activity of catalysts in Library III from the activity screening with eight tubular flow reactors at (a) 400°C, (b) 450°C, and (c) 500°C.

Figure 4.35 Contour plots of activity of catalysts in Library III from the activity screening with eight tubular flow reactors at (a) 550°C, (b) 600°C, and (c) 800°C.

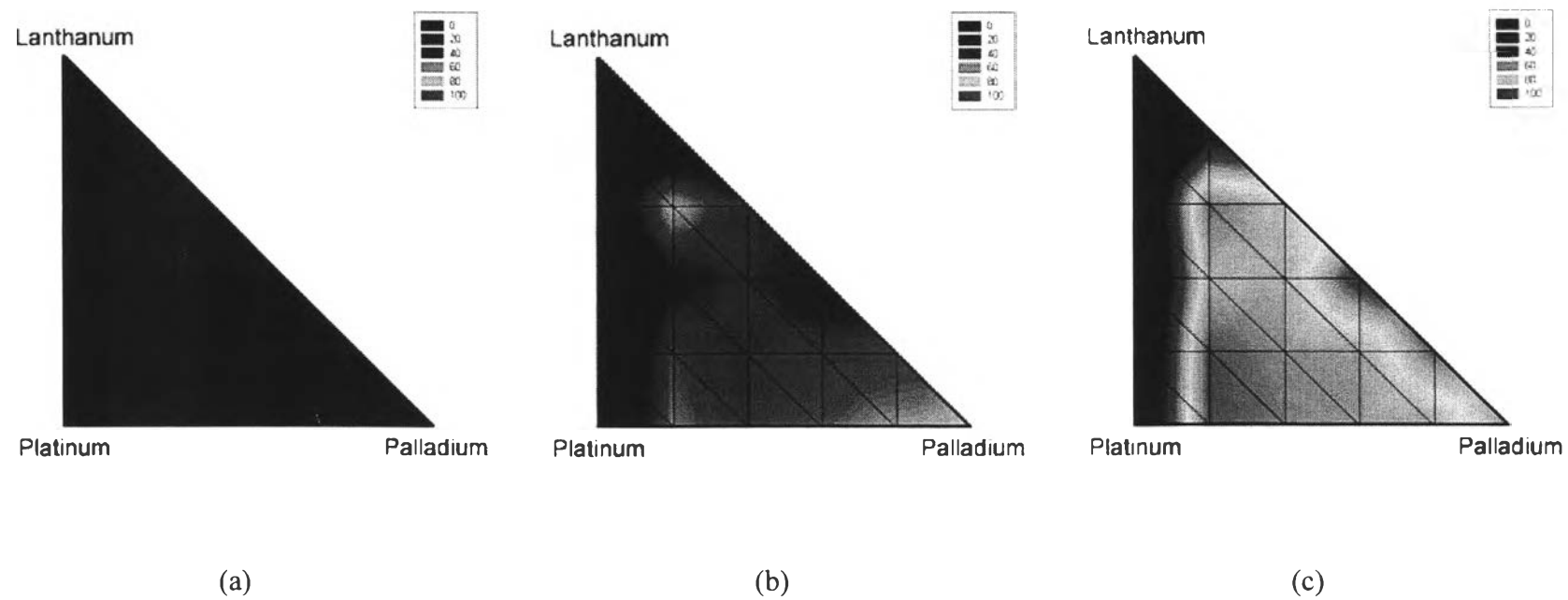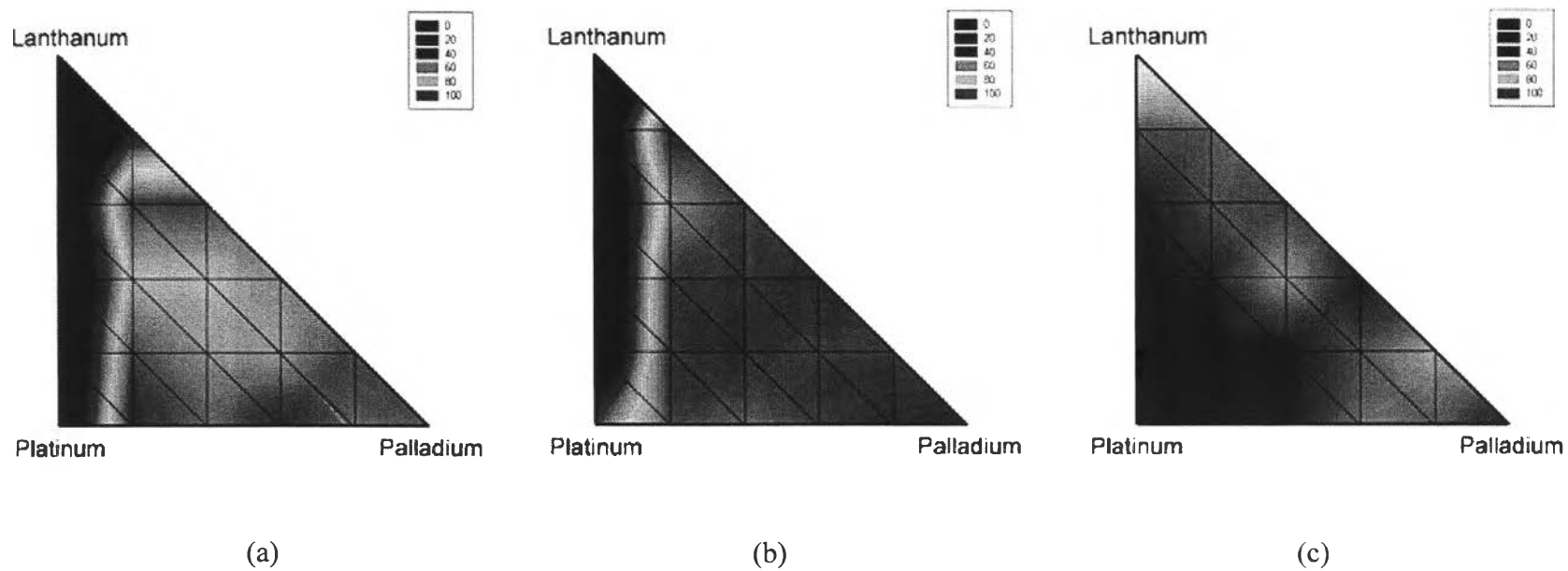Since the main purpose of this research is to find the catalysts that can be used in the low-temperature section of a hybrid designed combustor (450-550°C). The criterion for making a decision to select the lead formulation has to be based on the real obligation of the low-temperature catalyst, which aims to partially combust a lean mixture of fuel. Thus, the catalyst with conversion of about 70% was selected as the lead formulations since this much conversion can ensure an enough combust activity under the higher linear velocity condition, which is the operating condition of a commercialized gas turbine.

The contour plot at 400°C (Figure 4.34a) indicates a low potential of methane combustion on catalytic surface since less than 40% conversion were observed for all catalysts. When the temperature was increased to 450°C, as illustrated in Figure 4.34b, only catalyst containing relatively 20%Pd, 20%Pt and 60%La (C10) shows the outstanding activity around of 70% conversion, and was also selected as the first lead. Subsequently, other catalysts containing relatively 20%Pd in various amounts of Pt and La were also selected as the leads due to their higher conversion than 70% at about 500°C, as shown in Figure 4.34c. The active area was also developed on the Pd-Pt bi-element and Pd mono-element corners when the temperature was increased to 550°C (Figure 4.35a). As a result, the compositions of leads were listed in Table 4.4 and also shown in Figure 4.36.

For the catalytic activity investigated under overheating condition at about 800°C, some homogeneous combustion were observed as expected since at least 12% conversion of methane has been observed from the reaction without catalyst. Almost 100% conversion of all loaded catalysts was achieved at this high temperature.

In conclusion, these leads were categorized into two main groups: Pd-Pt bi-element catalysts, and Pd-Pt-La tri-element catalysts with relatively constant 20%Pd (equivalent to 1%Pd of 5% total elemental loading), for the further characterizations.

Table 4.4 Lead formulations selected from the activity screening results with the eight tubular flow reactors

No.	Catalyst	Ratio of element loading (%)		
		Pd	Pt	La
1	C10	20	20	60
2	C09	20	40	40
3	C08	20	60	20
4	C07	20	80	-
5	C12	40	60	-
6	C16	60	40	-
7	C19	80	20	-
8	C21	100	-	-

Lanthanum

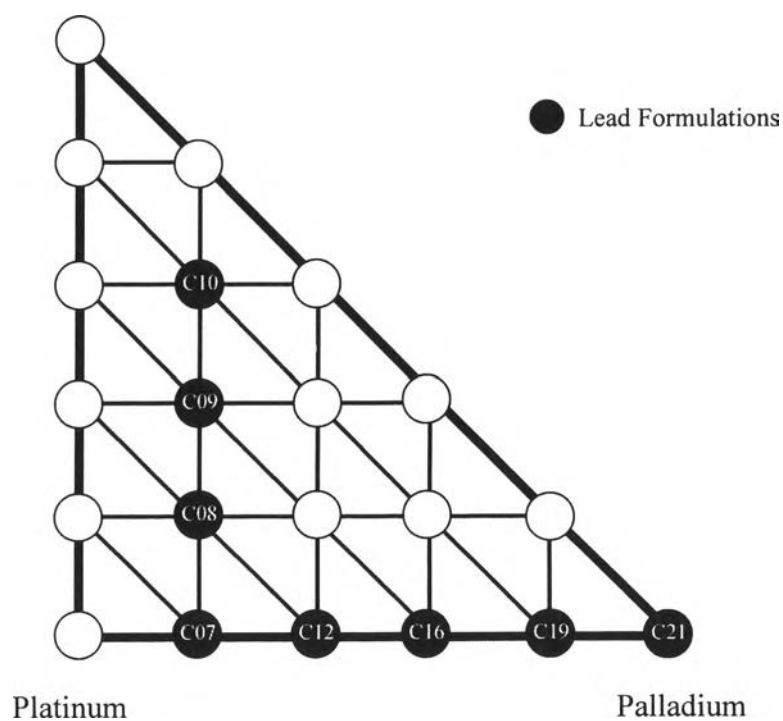Platinum   Palladium

Figure 4.36 A rightangled triangle tertiary diagram representing a systematic arrangement of lead formulations.

4.3 Lead Characterizations

Eight catalysts selected as leads were characterized with XRD and TPO/MS in order to investigate how the elements deposit on the catalyst surface, and some synergistic effects due to the use of elements in bi-, and tri-element system related to the combustion activity screened from the eight tubular flow reactors. The other two catalysts contained pure Pt and La were also selected to study and characterize as mono-element (pure loaded) catalysts.

4.3.1 X-ray Diffraction (XRD)

All XRD patterns of leads are illustrated in Figure 4.37. The patterns of three pure loaded catalysts indicate the existing phases in the case of pure loading. No additional peak observed for La/Al$_2$O$_3$ indicates that La is not present as a crystal cluster on the catalytic surface. It seems that La diffused into Al$_2$O$_3$ matrix, forming a solid solution. Both Pt and Pd are still present on catalytic surface, but in the different forms. Metallic Pt is identified at 39.7° of 2θ while PdO is observed from the 2θ peak at 33.8° in the XRD pattern of Pt/Al$_2$O$_3$ and Pd/Al$_2$O$_3$, respectively.

For the Pd-Pt bi-element catalysts, the substitution of Pd by Pt is observed to reduce the intensity of PdO peaks, moreover, the new peak whose 2θ is shifted into the region between the diffraction of Pt (39.7°) and Pd (40.1°) appears. This peak is expected to be the combination peak between metallic Pt and Pd similarly to the results of Ozawa *et al.* (2003). These observations also indicate that the substitution of Pd supported Al$_2$O$_3$ by Pt causes the alloy formation between metallic Pd and Pt. When the relative amount of substituted Pt is not higher than 60%, XRD analysis indicates that both PdO and Pd-Pt alloy were co-existed on the catalytic surface whereas only Pd-Pt and Pt-like pattern are observed when Pt was substituted in the higher amount (the PdO peak disappears).

For the tri-element leads, the substitution of Pt by La tends to decrease the Pd-Pt diffraction peak intensity due to the dilution of alloy by La. The interesting XRD pattern is observed in the case of adding Pd and Pt in equivalent weight ratio with three times of dilution by La (see C10) since a little peak of PdO was observed to co-exist on the catalytic surface with Pd-Pt alloy.
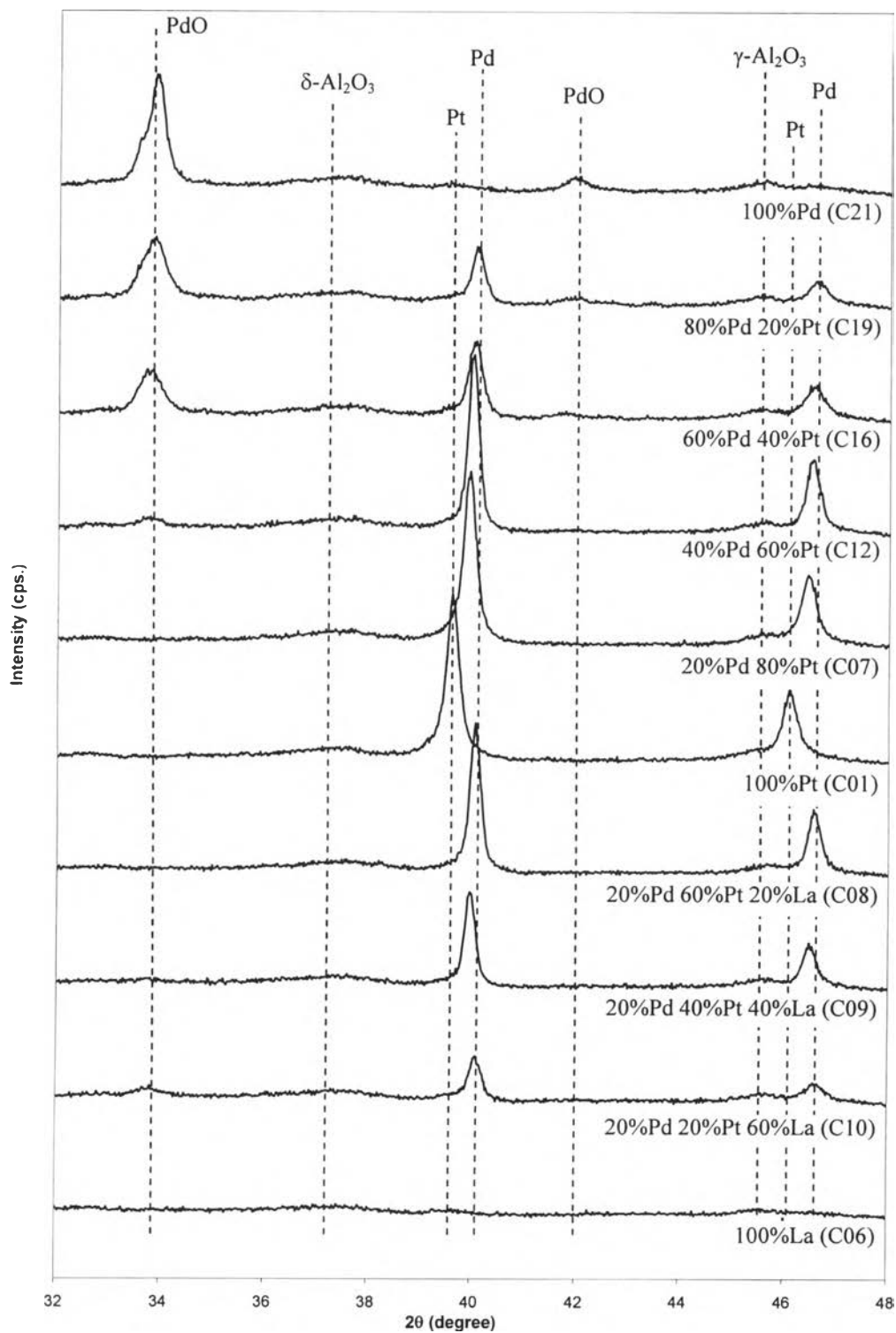
Figure 4.37 XRD patterns of fresh leads after calcined at 900°C for 3 hrs.

4.3.2 Temperature Programmed Oxidation (TPO)

In order to investigate the oxygen desorption temperature affected from using Pd, Pt and La in bi- and tri-element system, temperature programmed oxidation (TPO) of leads were performed, and the results are illustrated in Figure 4.38. The pure Pd catalyst shows 2 peaks of O_2 desorption at around 770°C and 815°C while pure La did not show any desorption peak. For pure Pt catalyst, a small O_2 consumption peak is observed at around 135°C without O_2 desorption at higher temperature as observed on the pure Pd catalyst.

The substitution of Pd by Pt tends to reduce both O_2 desorption temperature and intensity. This may be resulted from the dilution of PdO by Pt, and also from the formation of an alloy of metallic Pd with Pt, as indicated in XRD patterns. The further substitution of Pt by La in tri-element leads did not show any difference in TPO profiles when compared with those of La-free. These observations also confirmed the XRD results that only Pd-Pt alloy was existed. However, when Pt was substituted by La until its remaining weight was equal to that of Pd, some O_2 desorption peak is observed at around 715°C while a small O_2 consumption peak is still existed at 158°C. It can be explained that both PdO and Pd-Pt alloy were co-existed on the La-Al_2O_3 solid solution surface when Pt was co-loaded in the equivalent amount of Pd with three times dilution by La (C10). Moreover, the shift of desorption temperature to the lower also indicates some synergistic effect between Pd-Pt-La co-loaded elements.

From both XRD and TPO results, the surface model of leads is proposed as illustrated in Figure 4.39.
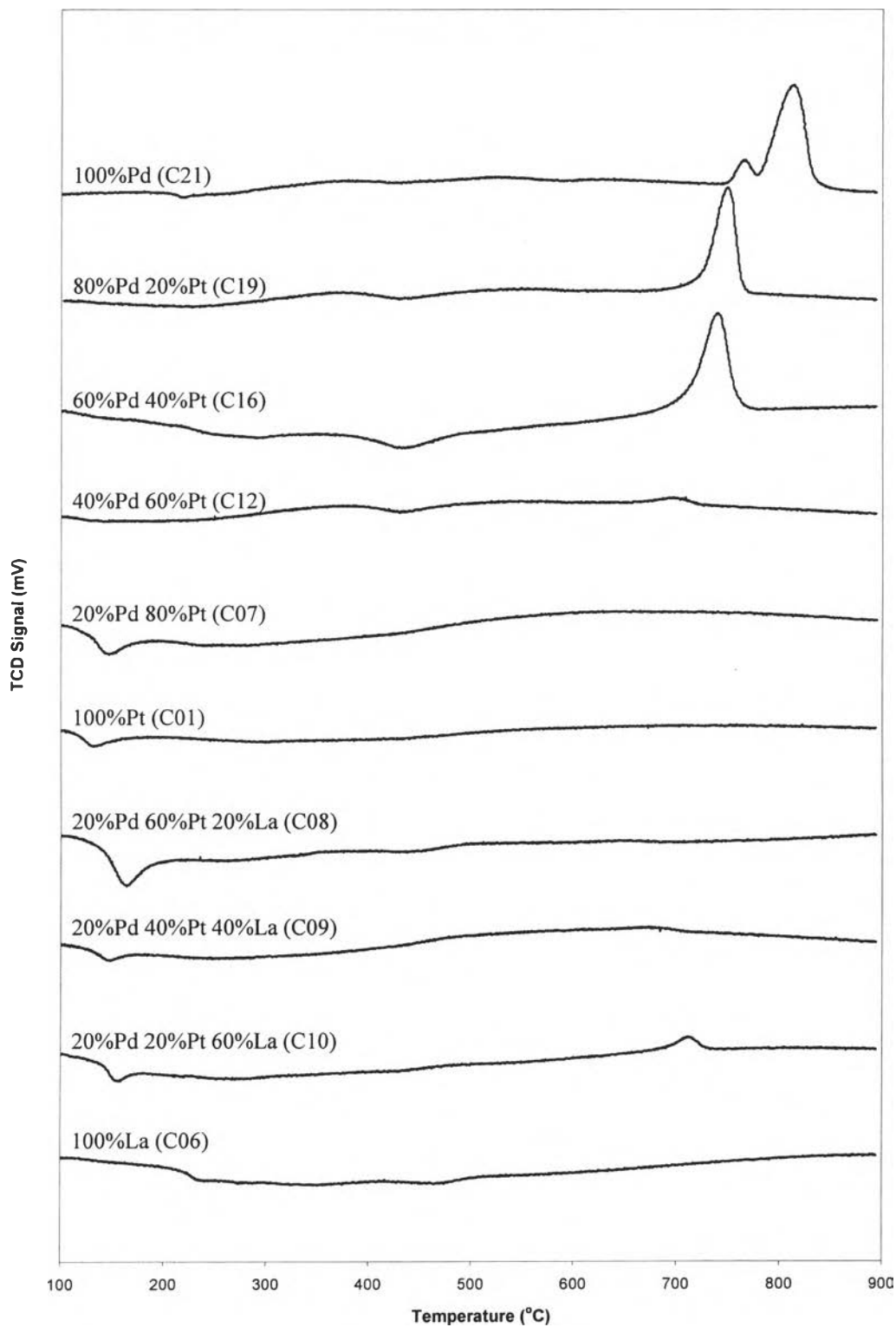
Figure 4.38 TPO profiles of fresh leads after calcined at 900°C for 3 hrs.
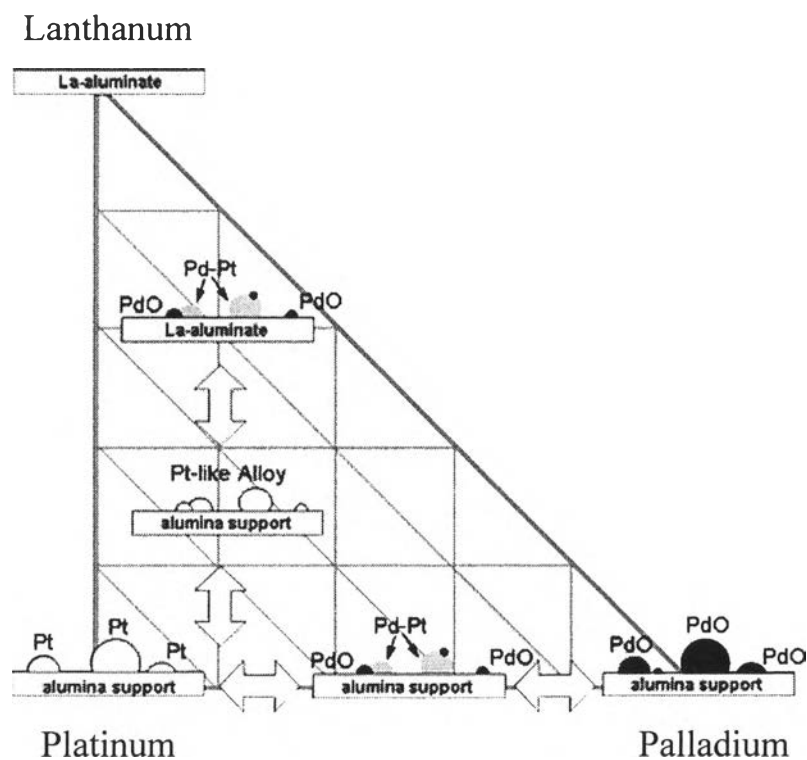
Lanthanum

Figure 4.39 Proposed surface models of leads suggested from XRD and TPO results.

All characterization data were used to explain what happened with the catalytic activity of leads when substituting Pd by Pt, and also subsequently substituting Pt by La. The methane conversions of leads are listed again in Table 4.5.

The substitution of Pd by Pt tends to increase the combustion activity at around 450-500°C. These results may be explained by the co-existence of PdO and Pd-Pt alloy as indicated by XRD. Since PdO dispersed on large crystallites of metallic Pd was reported to have a higher combustion activity than PdO dispersed on Al_2O_3 (Hicks *et al.*, 1990), the observation might suggest that the same phenomena could occur in our case. Ozawa *et al.* (2003) suggested that PdO would partially disperse on the large Pd-Pt crystallites at the initial and results in a higher TOF of Pd-Pt bi-element catalyst. Another reason that may explain the increase in activity is based on the dual site mechanism suggested by Su *et al.* (1998) and Carstens *et al.* (1998). Both metallic and oxide sites were believed to be active during the combustion, and both of them also co-existed in Pd-Pt bi-element system. The other

characteristic that might explain the enhancement of activity due to Pt substitution is the O_2 desorption temperature from TPO. The lower desorption temperature would mean the higher oxidation activity of catalyst due to the higher ability to release surface oxygen. The substitution of Pt seems to reduce this desorption temperature, indicating the increase of methane oxidation activity on the catalytic surface.

Table 4.5 Methane conversion[a] (%) at different temperatures of leads

No	Catalyst	Relative ratio of elemental loading[†] (%)			% Conversion at different temperatures (°C)					
		Pd	Pt	La	400	450	500	550	600	800
1	C21	100	-	-	32.3	60.7	56.8	88.8	97.0	100
2	C19	80	20	-	26.3	58.0	79.9	86.0	96.3	87.5
3	C16	60	40	-	10.5	52.1	82.2	96.8	93.4	85.5
4	C12	40	60	-	11.5	58.8	84.7	87.0	86.0	100
5	C07	20	80	-	12.1	56.6	91.6	97.7	89.9	100
6	C01	-	100	-	0.00	0.00	3.29	6.43	49.8	100
7	C08	20	60	20	11.2	53.3	89.9	87.4	89.6	100
8	C09	20	40	40	6.87	35.5	75.2	72.6	88.9	96.2
9	C10	20	20	60	11.6	64.5	86.3	89.9	76.9	87.5
10	C06	-	-	100	0.00	0.00	0.00	0.00	3.31	63.0

Note: [a] investigated at around 8 hrs time-on-stream
[†] with 5% total elemental loading

When Pd, Pt and La were co-loaded in tri-element system, the conversion of catalysts whose relative Pd loading percentage was controlled at about 20% was observed to slightly decrease with the amount of substituted La at low temperatures. This may be resulted from the dilution of noble metal presented on catalytic surface by La. However, when La continued diluting until the relative Pt remaining weight was equal to the weight of Pd (20% Pd, 20% Pt and 60% La, or C10), its combustion activity was slightly increased, and also higher than those of the other tri-element leads. Even though the combustion activity of this catalyst was not higher than that

of the bi-element lead (C07), its combustion activity was still higher than those of the bi-element catalysts containing almost equal amounts of Pd and Pt (C16 and C17) and also high enough to ensure the partial combustion under the high linear velocity condition. Therefore, it is selected as the best catalyst. As shown in the TPO profile of C10, the oxygen desorption peak occurs at the lowest temperature as compared with those of all catalysts, indicating that La might help releasing oxygen or providing oxygen during combustion and resulting in higher conversion. Both XRD and TPO results indicate the co-existence of PdO and Pd-Pt as similar as in Pd-Pt bi-element system, but supported on $LaAlO_3$ solid solution. Some synergistic effect might be expected to occur among Pd, Pt, and La since the combustion activity was higher.

Therefore, the best composition is Pd:Pt:La equal to 1:1:3 (C10). La addition in the tri-element system not only gives high CH_4 conversion, but also reduces the usage of expensive noble metals.